The International Journal of Biochemistry & Cell Biology 81 (2016) 335–345

Contents lists available at ScienceDirect

The International Journal of Biochemistry & Cell Biology

journal homepage: www.elsevier.com/locate/biocel

Original research

Diabetes impairs heart mitochondrial function without changes in resting cardiac performance

Silvina S. Bombicino[a], Darío E. Iglesias[a], Ivana A. Rukavina Mikusic[a], Verónica D'Annunzio[b], Ricardo J. Gelpi[b], Alberto Boveris[a], Laura B. Valdez[a,*]

[a] University of Buenos Aires, Institute of Biochemistry and Molecular Medicine (IBIMOL; UBA-CONICET), School of Pharmacy and Biochemistry, Physical Chemistry Division, Buenos Aires, Argentina
[b] University of Buenos Aires, Institute of Biochemistry and Molecular Medicine (IBIMOL; UBA-CONICET), Faculty of Medicine, Buenos Aires, Argentina

ARTICLE INFO

Article history:
Received 11 July 2016
Received in revised form
15 September 2016
Accepted 24 September 2016
Available online 25 September 2016

Keywords:
Type I diabetes
Streptozotocin (STZ)
Cardiac and mitochondrial dysfunction
Mitochondrial nitric oxide synthase (mtNOS)
Oxidative stress
Isoproterenol (ISO)

ABSTRACT

Diabetes is a chronic disease associated to a cardiac contractile dysfunction that is not attributable to underlying coronary artery disease or hypertension, and could be consequence of a progressive deterioration of mitochondrial function. We hypothesized that impaired mitochondrial function precedes Diabetic Cardiomyopathy. Thus, the aim of this work was to study the cardiac performance and heart mitochondrial function of diabetic rats, using an experimental model of type I Diabetes. Rats were sacrificed after 28 days of Streptozotocin injection (STZ, 60 mg kg^{-1}, *ip.*). Heart O_2 consumption was declined, mainly due to the impairment of mitochondrial O_2 uptake. The mitochondrial dysfunction observed in diabetic animals included the reduction of state 3 respiration (22%), the decline of ADP/O ratio (~15%) and the decrease of the respiratory complexes activities (22–26%). An enhancement in mitochondrial H_2O_2 (127%) and NO (23%) production rates and in tyrosine nitration (58%) were observed in heart of diabetic rats, with a decrease in Mn-SOD activity (~50%). Moreover, a decrease in contractile response (38%), inotropic (37%) and lusitropic (58%) reserves were observed in diabetic rats only after a β-adrenergic stimulus. Therefore, in conditions of sustained hyperglycemia, heart mitochondrial O_2 consumption and oxidative phosphorylation efficiency are decreased, and H_2O_2 and NO productions are increased, leading to a cardiac compromise against a work overload. This mitochondrial impairment was detected in the absence of heart hypertrophy and of resting cardiac performance changes, suggesting that mitochondrial dysfunction could precede the onset of diabetic cardiac failure, being H_2O_2, NO and ATP the molecules probably involved in mitochondrion-cytosol signalling.

1. Introduction

Diabetes Mellitus is a chronic metabolic disease characterized by an increase in blood glucose levels, which could be developed as a result of defects in insulin secretion, insulin action, or both. Hyperglycemia itself is a well-recognized risk factor for developing heart failure (Boudina and Dale Abel, 2007). Glucose uptake into the cardiomyocytes occurs through the glucose transporter GLUT-4, which is recruited to the cell membrane in response to insulin and expressed exclusively in insulin-sensitive tissues, such as skeletal muscle, adipose tissue and heart (Belke et al., 2001). Particularly, chronic Diabetes leads to a cardiac contractile dysfunction that is not attributable to underlying coronary artery disease or hypertension, and could be consequence of a progressive deterioration of mitochondrial function and bioenergetics (Ferreira et al., 2003; Fitzl et al., 2002; Pierce and Dhalla, 1985; Rolo and Palmeira, 2006). Moreover, the heart of diabetic patients is continuously exposed to high glucose and fatty acids concentrations, generating an oxidative environment (Aon et al., 2015; Rolo and Palmeira, 2006).

Mitochondria generate 95% of cellular ATP by oxidative phosphorylation, supplying the cardiomyocytes with the energy needed to maintain normal contractile function. In addition, mitochondria are the most important subcellular sites of reactive oxygen species production. Whereas increased reactive oxygen generation has been shown in endothelial cells that had been exposed to hyperglycemia (Brownlee, 1995), few studies to date have included the

Abbreviations: ADP, adenosine diphosphate; H_2O_2, hydrogen peroxide; ISO, isoproterenol; mtNOS, mitochondrial nitric oxide synthase; NO, nitric oxide; O_2^-, superoxide anion; $ONOO^-$, peroxynitrite anion; STZ, Streptozotocin.

* Corresponding author at: Cátedra de Fisicoquímica, Facultad de Farmacia y Bioquímica, Universidad de Buenos Aires, Junín 956, C1113AAD, 2o piso, Buenos Aires, Argentina.
E-mail addresses: lbvaldez@ffyb.uba.ar, laubeaval@gmail.com (L.B. Valdez).

http://dx.doi.org/10.1016/j.biocel.2016.09.018
1357-2725/

quantification of oxygen and nitrogen reactive species produced by heart mitochondria using experimental models of type I Diabetes (Bugger et al., 2008; Tocchetti et al., 2015).

Mitochondrial reactive oxygen and nitrogen species are mainly derived from two primary free radicals: superoxide anion (O_2^-) and nitric oxide (NO). Superoxide anion is the precursor of hydrogen peroxide (H_2O_2) and is generated within mitochondria through the autoxidation of the intermediate semiquinones ($UQH^\bullet$ and $FMNH^\bullet$) of the redox pairs ubiquinol/ubiquinone (complex III) and $FMNH_2$/FMN component of the NADH dehydrogenase (complex I) (Boveris et al., 1972; Boveris and Cadenas, 1975; Turrens and Boveris, 1980). In addition, mitochondrial NO is produced through the reaction catalyzed by mitochondrial nitric oxide synthase (mtNOS), an isoenzyme of the NOS family located in the inner mitochondrial membrane (Giulivi, 1998; Giulivi et al., 1998; Tatoyan and Giulivi, 1998) and identified as the α-nNOS with post-translational modifications (Elfering et al., 2002). Mitochondrial NOS expression and activity are highly regulated (Bombicino et al., 2016b; Boveris et al., 2002, 2006; Valdez et al., 2006) and, in turn, the NO inhibits mitochondrial respiration through its effects on the respiratory complex IV (Antunes et al., 2004, 2007; Brown and Cooper, 1994; Cleeter et al., 1994) and complex III (Iglesias et al., 2015; Poderoso et al., 1996), modifying the O_2^- and H_2O_2 mitochondrial production rates. Nitric oxide also reacts with O_2^- through a controlled diffusion reaction ($\sim 2 \times 10^{10}\ M^{-1}\ s^{-1}$) yielding $ONOO^-$ (Kissner et al., 1997; Radi et al., 2002; Valdez et al., 2000). At present, H_2O_2 and NO are considered mitochondrion-cytosol signalling molecules because of they are involved in the modulation of redox-sensitive kinase signalling and transcriptional pathways (Jones and Sies, 2015; Sies, 2015; Yin et al., 2012; Yin et al., 2014; Yin and Cadenas, 2015). The molecular signals could play a central contribution in the onset, progression and/or pathological consequences of Diabetes.

Therefore, the aim of this work was to study the cardiac performance and its association with mitochondrial function, using an experimental model of type I Diabetes Mellitus, in which the hyperglycemia occurs without the presence of the typical type 2 Diabetes characteristics, *i.e.* insulin resistance, obesity, hypercholesterolemia and hypertension.

2. Materials and methods

2.1. Drugs and chemicals

Streptozotocin (STZ, S0130) and other chemicals were purchased from Sigma Chemical Co. (St. Louis, MO, USA). Anti-nitrotyrosine antibodies (HM.11, sc-32731) were from Santa Cruz Biotechnology (Santa Cruz, CA). Other reagents were of analytical grade.

2.2. Experimental design

Male Wistar rats of about 6–7 weeks from birth (200–220 g) were housed in separate cages in an environmentally controlled facility at 25 °C. The animals were subjected to circadian light–dark cycles, fed standard rat chow, and provided water *ad libitum*. The procedures used in this study were approved by the Animal Care and Research Committee of the School of Pharmacy and Biochemistry, University of Buenos Aires (CICUAL; Exp. 00663658/15), and this investigation was in accordance with the International Guiding Principles for Biomedical Involving Animals (ICLAS).

Rats were divided in two groups, *Diabetes Mellitus* (DM) and *Control* (C). Diabetes was induced by a single dose of Streptozotocin (STZ, 60 mg kg^{-1} animal weight, *ip.*) diluted in citrate buffer 100 mM pH 4.50. Control group was injected with the vehicle (citrate buffer 100 mM pH 4.50; 1 ml kg^{-1}, *ip.*) (Li et al., 2009; Rossini et al., 1977). Rats were considered diabetics if their fasting blood glucose values, 3 days after the STZ administration, were higher than 200 mg dl^{-1}, being this latter the cut off value to consider the animals as diabetics (Joffe et al., 1999). From the beginning of the treatment, the animals were weighed once a week. After 28 days of STZ-injection, glucose values were tested, animals were sacrificed in a CO_2 atmosphere and hearts were removed. All the experimental procedures were performed using the whole heart.

3. Sample preparation

3.1. Isolated heart perfusion

Hearts were excised and placed in a perfusion system according to the Langendorff technique. Perfusion medium consisted in a Krebs-Henseleit buffer containing 118 mM NaCl, 4.7 mM KCl, 1.2 mM KH_2PO_4, 1.2 mM $MgSO_4$, 2.5 mM $CaCl_2$, 25 mM $NaHCO_3$ and 10 mM glucose, pH 7.40, equilibrated with 95% O_2/5% CO_2 at 37 °C. Two electrodes were sutured and connected to a pacemaker in order to stimulate the heart and to maintain a constant heart rate of 250–300 beats min^{-1}. A latex balloon connected to a pressure transducer (Deltram II; Utah Medical System) via a polyethylene cannula was inserted into the left ventricle (LV) for measurement of LV pressure. The latex balloon was filled with distilled water to achieve a left-ventricle end-diastolic pressure (LVEDP) of 8–10 mm Hg. All hearts were perfused with constant coronary flow (13 ml min^{-1}) to obtain a coronary perfusion pressure of 70.5 ± 4.2 mmHg during the initial stabilization period that was kept constant throughout the experiment. Left-ventricular pressure was recorded in real time using a computer with data acquisition hardware (Utah Medical System, UT, USA).

3.2. Tissue cubes preparation

Hearts were isolated, washed, weighed and kept in Krebs-Henseleit buffer, at 4 °C. Then, 1 mm^3 tissue cubes were cut by the use of a scalpel (Navarro et al., 2005). The average weight of the cubes was 1.0 mg $cube^{-1}$.

3.3. Heart mitochondrial isolation and mitochondrial membranes preparation

Heart mitochondrial fraction was obtained from tissue homogenates by differential centrifugation in a Sorvall RC5C centrifuge (Sorvall-Instruments-Du Pont, Model RC5S, Buckinghamshire, England). The hearts were isolated, washed, and minced in 5 ml of ice-cold medium containing 250 mM sucrose, 2 mM EGTA, 5 mM Tris-HCl, pH 7.40 (STE-1). This procedure was repeated and then the sample was divided in two petri dishes; in one of them the buffer was removed and filled with a buffer containing STE added with 0.5% (w/v) BSA, 5 mM $MgCl_2$, 1 mM ATP and 2.5 U ml^{-1} type XXIV bacterial proteinase, pH 7.40 (STE-2). After 4 min of incubation at 4 °C, both samples were homogenized in 1:10 STE-1 buffer with a glass-Teflon homogenizer and centrifuged at 8000*g* for 10 min. The pellet was resuspended in ice-cold STE-1 buffer and centrifuged at 700*g* for 10 min. The sediment was discarded and both supernatants were mixed and centrifuged at 8000*g* for 10 min. The pellet of this centrifugation was resuspended in STE-1 buffer and centrifuged at 8000*g* for 10 min. The pellet containing the mitochondrial fraction was rinsed and resuspended in STE-1 buffer. The whole procedure was carried out al 0–4 °C (Iglesias et al., 2015; Mela and Seitz, 1979). Protein concentration was determined with the Folin reagent (Lowry et al., 1951) using bovine serum albumin as standard.

Mitochondrial membranes were obtained by three cycles of freezing and thawing of the mitochondrial preparation and homogenized by passage through a 25-gauge hypodermic needle (Boveris et al., 2002).

4. Cardiac performance

4.1. Systolic and diastolic ventricular function

Systolic and diastolic functions were assessed both at baseline and after a β-adrenergic stimulus through the addition of 1 μM isoproterenol (ISO) to the perfusion medium. This experimental strategy allows evaluating the myocardial reserve, *i.e.* the capacity of the heart to respond to an additional metabolic requirement (Jain et al., 2001). The β-adrenergic stimulus leads to positive inotropic and lusitropic effects, like an increase in the contraction force and in the myocardium relaxation rate, respectively, similarly to a cardiac work overload (Sicari et al., 2008).

Systolic behaviour was evaluated as left-ventricular developed pressure (LVDP, calculated as the difference between peak systolic pressure and LVEDP) and also with the maximum rate of increase of the intraventricular pressure ($+dP/dt_{máx}$), both contractile state indexes. The isovolumic relaxation (lusitropism) was analyzed as the time required for the left ventricular pressure to fall up to 50% from the peak of LVDP (t_{50} or relaxation rate). Thus, a higher relaxation rate correlates with a lower time to reach 50% of relaxation (t_{50}) (Marchini et al., 2013; Vittone et al., 1974). The addition of β-agonists, such as isoproterenol, leads to an increment in the relaxation velocity, *i.e.* a lower value of t_{50}.

4.2. Heart O_2 uptake

Tissue O_2 uptake rates were determined polarographically, at 30 °C, using a Clark-type electrode (Hansatech Oxygraph, Hansatech Instruments Ltd, Norfolk, England). Hearts were sectioned into 1 mm^3 cubes; and two to four cubes were added to 1.0 ml of Krebs-Henseleit buffer. Initial O_2 consumption rates (up to 8–10 min) showed a linear relationship with tissue mass (Valdez et al., 2011). In order to estimate the amount of O_2 consumed by mitochondria, 2 mM KCN was added to the reaction chamber, after 3 min of tissue addition, to inhibit the cytochrome oxidase of the mitochondrial respiratory chain. By this approach, the fraction inhibited by KCN corresponds to mitochondrial O_2 consumption, and the remainder O_2 uptake corresponds to the O_2 consumed by other cellular sources, such as peroxidases and oxidases, *e.g.* NAPDH oxidase, and non-enzymatic autoxidation reactions (Ernster, 1986; Pesta and Gnaiger, 2012). The results were expressed as μmol O_2 min^{-1} g $tissue^{-1}$.

5. Mitochondrial function

5.1. Mitochondrial O_2 consumption and oxidative phosphorylation efficiency (ADP/O)

Mitochondrial O_2 uptake was followed polarographically with a Clark-type electrode (Hansatech Oxygraph, Hansatech Instruments Ltd, Norfolk, England). State 4 respiration was determined at 30 °C in an air-saturated (220 μM O_2) reaction medium consisting of 120 mM KCl, 5 mM KH_2PO_4, 1 mM EGTA, 3 mM HEPES, 1 mg ml^{-1} BSA, 2 mM malate and 5 mM glutamate (complex I substrates) or 5 mM succinate (complex II substrate), pH 7.20, and heart mitochondrial suspension (0.1–0.3 mg mitochondrial protein ml^{-1}). State 3 O_2 consumption rate was established by supplementation of this medium with 0.5 mM ADP (Boveris et al., 1999). Results were expressed as ng-at O min^{-1} mg $protein^{-1}$ and the respiratory control ratio (RC) was calculated as the ratio of state 3/state 4 respiration rates.

In order to estimate the efficiency of the oxidative phosphorylation through the number of moles of phosphate equivalents esterified per oxygen consumed (ADP/O ratio), state 3 O_2 consumption was established by the addition of limiting amounts of ADP (0.2 mM). ADP/O ratio was calculated considering the amount of O_2 that is consumed during mitochondrial state 3 and the concentration of ADP added to the chamber (Estabrook, 1967). Taking into account the relation 1:1 for the formation of ATP per each ADP consumed, the amount of nmol of ATP produced per ng-atom of oxygen consumed was calculated. The results are expressed as nmol ATP ng-atom O^{-1}.

5.2. Mitochondrial electron transfer activities

Respiratory chain complexes (I–III, II–III, and IV) activities were determined spectrophotometrically using a Beckman DU 7400 diode array spectrophotometer, at 30 °C (Navarro et al., 2005; Valdez et al., 2011; Zaobornyj et al., 2009).

Complex I–III was determined as NADH-cytochrome *c* reductase activity and complex II–III was determined as succinate-cytochrome *c* reductase activity, following the reduction of cytochrome c^{3+} at 550 nm (ε = 19 mM^{-1} cm^{-1}) (Hatefi, 1985). Mitochondrial membranes suspended in 100 mM KH_2PO_4/K_2HPO_4 pH 7.40 (0.01–0.03 mg protein ml^{-1}) were added with 0.2 mM NADH or 6.0 mM succinate as substrates, 25 μM cytochrome c^{3+}, and 0.5 mM KCN. Enzymatic activities were expressed as nmol of reduced cytochrome c^{3+} min^{-1} mg $protein^{-1}$.

Complex IV activity (cytochrome oxidase) was determined in mitochondrial membranes suspended in 100 mM KH_2PO_4/K_2HPO_4 pH 7.40 (0.01–0.03 mg protein ml^{-1}) and supplemented with 50 μM cytochrome c^{2+} (Yonetani and Ray, 1965; Yonetani, 1967). The rate of cytochrome c^{2+} oxidation by complex IV was calculated as the pseudo-first-order reaction constant (k′) and expressed as min^{-1}mg $protein^{-1}$. Reduced cytochrome *c* was freshly prepared by reduction of cytochrome c^{3+} with $Na_2S_2O_4$, followed by Sephadex G-25 chromatography. In order to test the reduction of cytochrome *c* solution, the ratio between absorbances at 550 nm and at 565 nm (A_{550nm}/A_{565nm}) was calculated. The cytochrome *c* solution was used to measure complex IV activity in the samples if this ratio was higher than 6, indicating an adequate proportion of cytochrome c^{2+}. The concentration of cytochrome c^{2+} solution (about 0.8–1.0 mM) was calculated from the absorbance at 550 nm (ε = 19 mM^{-1} cm^{-1}).

5.3. Hydrogen peroxide production

Mitochondrial H_2O_2 production was determined fluorometrically at 365–450 nm ($\lambda_{exc\text{-}em}$) using a Hitachi F-3010 fluorescence spectrophotometer, at 30 °C, through the scopoletin–horseradish peroxidase (HRP) assay (Boveris, 1984). The reaction medium consisted of 0.23 M mannitol, 0.07 M sucrose, 20 mM Tris–HCl, pH 7.40, added with 0.5 μM Cu,Zn-SOD, 1 μM HRP, 1 μM scopoletin and mitochondrial suspensions (0.1–0.3 mg protein ml^{-1}). Mitochondrial H_2O_2 production rates were determined in state 4 using 6 mM malate and 6 mM glutamate or 8 mM succinate as substrates of complex I or II, respectively. To distinguish the H_2O_2 production associated with O_2^- generation from complex I, H_2O_2 production rates were determined in the absence or in the presence of 1 μM rotenone. A calibration curve was made using H_2O_2 (0.05–0.35 μM) as standard, previously titrated spectrophotometrically at 240 nm (ε = 43.6 M^{-1} cm^{-1}), to express the fluorescence changes as nmol H_2O_2 min^{-1} mg $protein^{-1}$.

5.4. Nitric oxide production

Nitric oxide production by mitochondrial membranes was measured at 37 °C, following the oxidation of oxyhemoglobin (HbO_2) to methemoglobin at 577–591 nm ($\varepsilon = 11.2\ mM^{-1}\ cm^{-1}$) using a Beckman DU 7400 diode array spectrophotometer (Boveris et al., 2002; Murphy and Noack, 1994; Valdez et al., 2011). The reaction medium consisted of 50 mM KH_2PO_4/K_2HPO_4, pH 7.40, 1 mM L-arginine, 1 mM $CaCl_2$, 100 μM NADPH, 10 μM dithiothreitol (DTT), 4 μM Cu,Zn-SOD, 0.1 μM catalase, 20 μM HbO_2 heme, and the mitochondrial membranes suspension (0.15–0.25 mg protein ml^{-1}). In order to consider only the L-NMMA-sensitive HbO_2 oxidation, control experiments adding the inhibitor of mtNOS L-NMMA (2 mM) were performed. The absorbance changes that were inhibited by L-NMMA were expressed as nmol NO min^{-1} mg $protein^{-1}$.

5.5. Nitrotyrosine detection by western blot

Equal amount of mitochondrial membranes (80 μg protein) were subjected to 7.5% sodium dodecyl sulfate–polyacrylamide gel electrophoresis. Non-specific binding was blocked by incubation of the membranes with 5% non-fat dry milk in PBS for 1 h at room temperature. The membranes were blotted into nitrocellulose films and probed with 1:100 diluted mouse monoclonal anti-nitrotyrosine antibody (HM.11, sc-32731 Santa Cruz Biotechnology, Santa Cruz, CA) or 1:500 diluted goat polyclonal anti-VDAC-1 antibody (D-16: sc-32063, Santa Cruz Biotechnology, Santa Cruz, CA). The nitrocellulose membranes were subsequently incubated with a secondary rabbit anti-mouse IgG antibody ((315-035-048) Jackson Inmuno Research, Baltimore Pike, USA) or a mouse anti-goat antibody (IgG-HRP, sc: 2354, Santa Cruz Biotechnology, Santa Cruz, CA) (dilution 1:5000), respectively. The secondary antibodies were conjugated with horseradish peroxidase and were revealed by chemiluminiscence with ECL reagent. Densitometric analysis of the bands was performed using the Image 1.62 software (Wayne Rasband, NIH, Bethesda, MD, USA) and data was expressed as relative to VDAC-1 expression (loading control) (Bustamante et al., 2002).

5.6. Mn-SOD activity and concentration

Manganese-superoxide dismutase (Mn-SOD) activity was assayed at 550–540 nm by monitoring the reduction rate of partially acetylated ferricytochrome c^{3+} ($\varepsilon = 19\ mM^{-1}\ cm^{-1}$) by the non-enzymatic reaction with O_2^- (Flohe and Gunzler, 1984; McCord and Fridovich, 1969; Valdez et al., 2011). The xanthine-xanthine oxidase system was used as O_2^- source. The reaction medium consisted of 50 mM KH_2PO_4/K_2HPO_4 added with 1 mM EDTA, pH 7.80 containing, 10 μM partially acetylated ferricytochrome c^{3+}, 50 μM xanthine, and sufficient xanthine oxidase (XO; ~5 nM) to reach an absorbance increase of 0.025 per min at 25 °C, in the absence of SOD. The reaction was started by the addition of xanthine and the absorbance was followed continuously for 2 min, in the absence or in the presence of different amounts of mitochondrial membranes suspension (2.5–30 μg ml^{-1}). One unit of SOD was defined as the amount of enzyme that inhibits by 50% the reduction of ferricytochrome *c* and corresponds to 4.0 pmol of Mn-SOD. Control experiments in the presence of 0.5 mM KCN were carried out to discount the inhibition of cytochrome *c* reduction associated with the CuZn-SOD activity. Under our experimental conditions, the addition of KCN to the reaction medium did not modify the rate of cytochrome *c* reduction. Results were expressed as Mn-SOD activity (U mg $protein^{-1}$) and as Mn-SOD concentration (μM) in the mitochondrial matrix.

6. Statistics

Results included in tables and figures are expressed as means ± SEM and represent replicated measurements on at least three to eight independent experiments.Student's *t*-test was used to analyse the significance of differences between Control and Diabetes groups. Values of $p < 0.05$ and $p < 0.01$ were considered statistically significant and highly significant, respectively. Statistical analysis was done using GraphPad Instat 4 (GraphPad Software, La Jolla, CA, USA).

7. Results

7.1. Rats and hearts weights and blood glucose concentrations

Rat blood glucose concentration after 3 days of STZ-injection was 423 ± 15 mg dl^{-1}, while control animals showed normal glycemia of 120 ± 5 mg dl^{-1}. Blood glucose values of both groups were maintained at the same level until the end of the treatment (Fig. 1A).

As previously reported (Mora et al., 2009; Tomita et al., 1996), the weight of control animals increased steadily along the 28 days (69%), in accordance to a normal growth profile for control animals in this period (Fig. 1B). However, diabetic rats did not increase their weight, after the instauration of Diabetes (Initial: 223 ± 4 g *vs.* 4 weeks: 257 ± 11 g). In accordance to this observation, hearts weights at day 28 were also lower in diabetic (0.89 ± 0.04 g) than in control (1.27 ± 0.04 g) animals (Fig. 1C), showing a linear correlation ($r^2 = 0.771$) between hearts and bodies weights. Although heart weight of diabetic rats was lower than the one of control rats, the cardiac index (Fig. 1D), calculated as the ratio between heart weight/animal weight, was not different between groups (C *vs* DM, 0.34 ± 0.04 *vs.* 0.36 ± 0.06), indicating that there is not heart hypertrophy in diabetic animals at the time studied.

7.2. Cardiac performance

7.2.1. Systolic and diastolic ventricular function

Systolic and diastolic ventricular functions were assessed both at baseline and after a β-adrenergic stimulus with isoproterenol. Fig. 2A shows that, at day 28, cardiac function measured as left-ventricular developed pressure (LVDP) in basal or resting conditions was similar in diabetic and control animals. While an enhancement of 52% was observed in LDVP of control group after perfusion with isoproterenol, the increase in LVDP was only about 32% in diabetics animals ($p < 0.05$). Interestingly, after a β-adrenergic stimulus, diabetic animals showed a lower contractile response (38%) compared to control animals (Fig. 2B).

A similar behaviour was observed in the maximal rate of increase of the intraventricular pressure ($+dP/dt_{máx}$) (Fig. 2C). The $+dP/dt_{máx}$ values were similar between groups at resting situation. However, after a β-adrenergic stimulus, the increase in $+dP/dt_{máx}$ observed in control hearts was about 87% while the enhancement in hearts from diabetic animals was 55%, suggesting a contractile reserve dysfunction in diabetic rats.

Left ventricular diastolic function was evaluated through the isovolumic relaxation index (t_{50}), which indicates the time needed to reach 50% of the maximum intraventricular pressure. A higher relaxation rate correlates with a lower time to reach 50% of relaxation. No differences between control and diabetic groups were observed in this parameter in resting conditions (Fig. 2E). However, when a β-adrenergic stimulus with isoproterenol was induced, hearts of control animals showed a reduction in t_{50} of 26%, increasing their relaxation rate, while hearts of diabetic rats showed a reduction of only 11%. Fig. 2F shows the difference between the

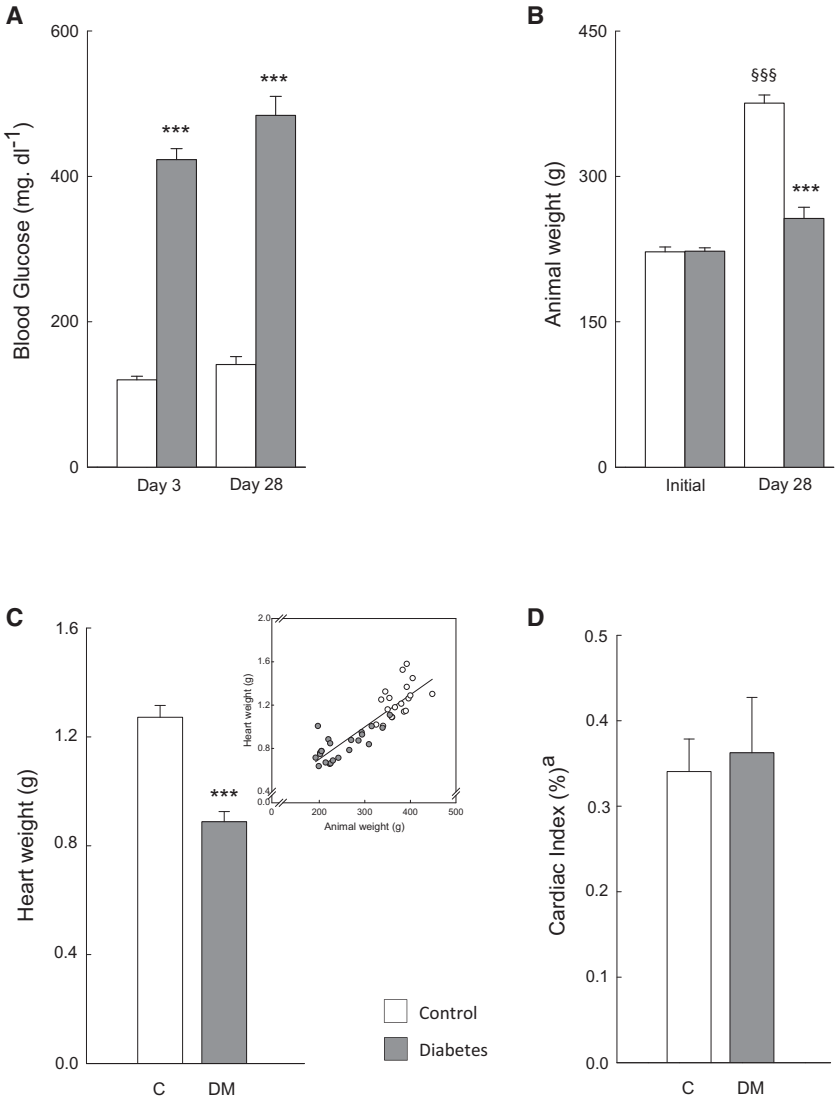

Fig. 1. (A) Blood glucose concentration of control and diabetic animals, 3 and 28 days after STZ-injection. (B) Animalís weight the day of the injection (initial) and at the end of the treatment (Day 28). (C) Heart weight. Inset: Linear correlation between heart weight and animal weight at the end of the treatment ($r^2 = 0.771$). (D) Cardiac index, calculated as the ratio between heart weight and animal weight at the end of the treatment. Control group (white bars or dots), Diabetic group (grey bars or dots). ***$p < 0.005$ Diabetes *vs.* control (Student's *t*-test; C n = 16; DM n = 25). §§§ $p < 0.005$ control (day 28) *vs.* control (initial) (Student's *t*-test; n = 16).

t_{50} values in basal conditions and after isoproterenol addition, expressed as a variation of time (Δt_{50}), and indicates that there is an impairment of the lusitropic reserve, or relaxation velocity, in hearts of diabetic animals (55%) in response to a work overload.

Consequently, the overall results show contractile and lusitropic reserve impairments in hearts obtained from diabetic animals, indicating a ventricular dysfunction evidenced only when hearts are exposed to a work overload and non-detected when heart works at resting conditions.

7.2.2. Heart oxygen consumption

Heart O_2 consumption rates were assessed in 1 mm^3 tissue cubes. Tissue O_2 uptake was slightly lower (12%) in diabetic animals than in control animals in basal conditions (Table 1). When KCN, which inhibits cytochrome oxidase activity, was added to the reaction chamber no differences in the remained O_2 uptake was observed. The O_2 uptake sensitive to KCN was significantly lower (18%) in hearts from diabetic than from control animals, suggesting that the decline in tissue O_2 consumption observed in STZ-injected animals is mainly due to a mitochondrial respiratory chain dysfunction.

Table 1
Heart O_2 uptake of control and STZ-induced diabetic rats.

Experimental conditions	Oxygen uptake (μmol O_2 min^{-1} g tissue^{-1})	
	Control	Diabetes
Basal	3.68 ± 0.14	3.24 ± 0.10*
+ KCN	1.20 ± 0.11	1.20 ± 0.12
Mitochondrial consumption	2.48 ± 0.18	2.04 ± 0.16*

* $p < 0.05$ Diabetes *vs.* Control (Student's *t*-test; n = 3).

7.3. Mitochondrial function

7.3.1. Mitochondrial O_2 consumption, electron transfer activities and oxidative phosphorylation efficiency

In order to evaluate mitochondrial function, we measured mitochondrial O_2 consumption, using malate-glutamate or succinate as substrates of complexes I or II, respectively (Table 2). State 3 mitochondrial respiration, the active respiration that yields ATP, was significantly decreased when malate-glutamate (22%) or succinate (17%) were used as substrates of complex I or II, respectively; while

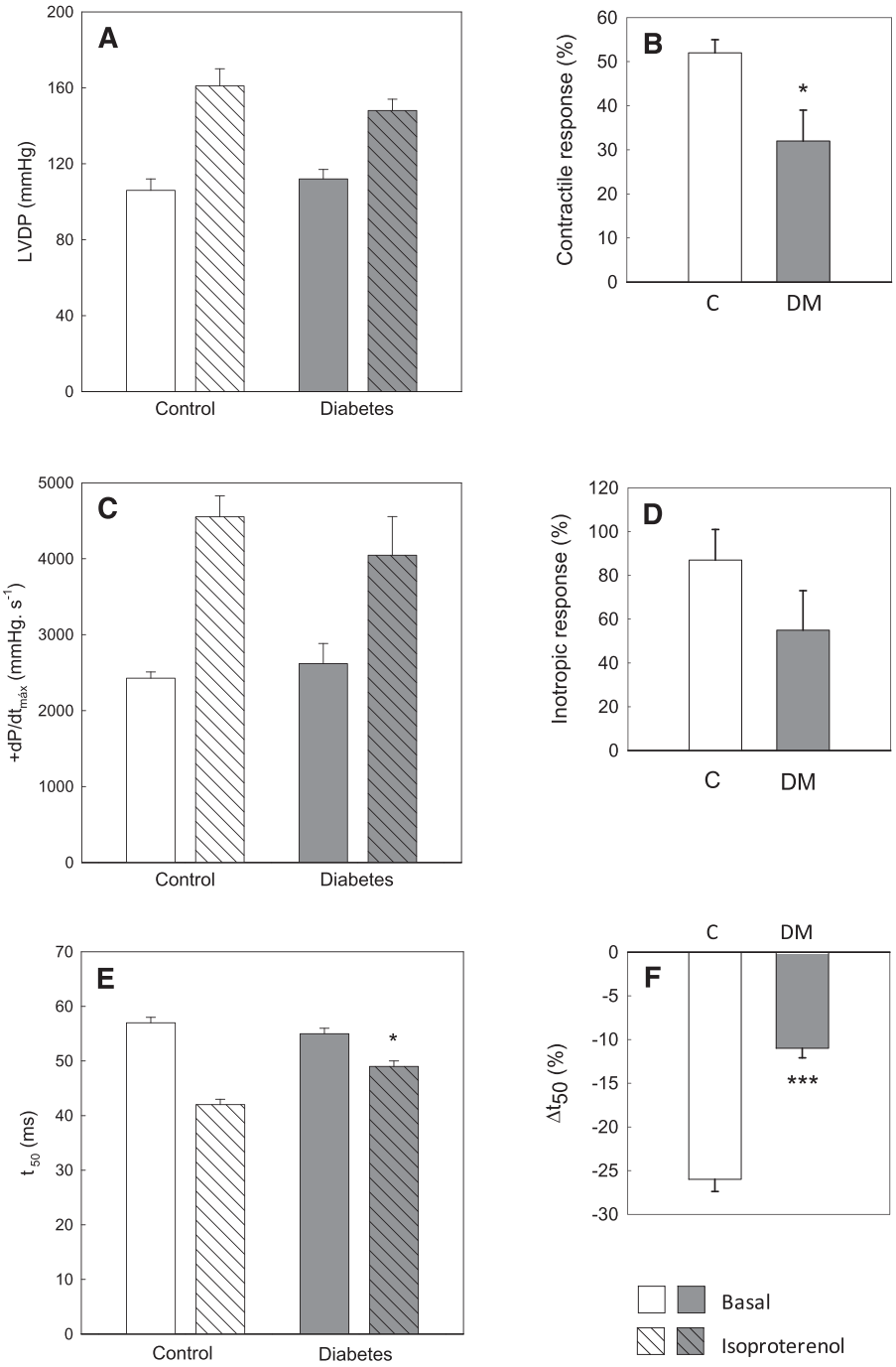

Fig. 2. Ventricular systolic function (A–D). (A) Left ventricular development pressure (LVDP) in basal conditions (full bars) and after stimulation with a β-adrenergic stimulus, isoproterenol (stripped bars). LVDP was calculated as the difference between peak systolic pressure and left ventricular end diastolic pressure (LVEDP). (B) Contractile response (%) calculated as the difference between LVDP after the β-adrenergic stimulus and LVDP in basal conditions, relative to basal LVDP. (C) First derivative of LV pressure (+$dP/dt_{máx}$) in basal conditions (full bars) and after stimulation with a β-adrenergic stimulus, isoproterenol (stripped bars). (D) Inotropic response (%) calculated as the difference between +$dP/dt_{máx}$ in the presence and in the absence of isoproterenol. Ventricular diastolic function (E and F). (E) Isovolumic relaxation time (t_{50}) measured as the time needed to reach 50% of relaxation in basal conditions (full bars) and after stimulation with isoproterenol (stripped bars). (F) Isovolumic relaxation (%) as an index of the lusitropic reserve capacity. $^{*}p < 0.05$; $^{***}p < 0.005$ Diabetes *vs.* Control group (Student's *t*-test).

the resting respiration (state 4) was not different between groups. The respiratory control ratio (RC), an estimator of mitochondrial integrity and of the coupling of the oxidative phosphorylation, was significantly declined (27%) in heart mitochondria from diabetic animals when the electrons enter by complex I of the respiratory chain. Moreover, the ADP/O ratio, an index of the oxidative phosphorylation efficiency, was significantly decreased (15%) when malate-glutamate was used as substrate.

The respiratory impairment of heart mitochondria form diabetic animals was further investigated by assaying mitochondrial respiratory chain complexes (Table 3). Complex I–III activity was 22% lower in diabetic animals than in control rats, being this difference highly significant. Additionally, complexes II–III (26%) and IV (22%) activities were also reduced in diabetic animals.

Table 2
Heart mitochondrial O_2 consumption and ADP/O ratio of control and STZ-induced diabetic rats.

	Mitochondrial O_2 uptake (ng–at O min^{-1} mg $protein^{-1}$)			ADP/O (nmol ng-$atom^{-1}$)
	State 4	State 3	Respiratory control	
		Malate-Glutamate		
Control	53 ± 8	217 ± 15	4.5 ± 0.2	2.71 ± 0.17
Diabetes	56 ± 6	169 ± 9*	3.3 ± 0.1*	2.30 ± 0.11*
		Succinate		
Control	117 ± 9	235 ± 10	2.0 ± 0.2	1.40 ± 0.16
Diabetes	114 ± 5	198 ± 9*	1.7 ± 0.1	1.25 ± 0.10

* $p < 0.05$ Diabetes *vs.* Control (Student's *t*-test; n = 8).

Table 3
Heart mitochondrial electron transfer activities of control and STZ-induced diabetic rats.

Group	Complex I–III (nmol min^{-1} mg $protein^{-1}$)	Complex II–III (nmol min^{-1} mg $protein^{-1}$)	Complex IV (min^{-1} mg $protein^{-1}$)
Control	492 ± 22	263 ± 17	60 ± 4
Diabetes	385 ± 16***	194 ± 13**	47 ± 3*

* $p < 0.05$. ** $p < 0.01$. *** $p < 0.005$ Diabetes *vs.* Control (Student's *t*-test, n = 6).

Table 4
State 4 mitochondrial H_2O_2 production and NO production rates of heart from control and STZ-induced diabetic rats.

Group	NO production (nmol min^{-1} mg $protein^{-1}$)	H_2O_2 production (nmol min^{-1} mg $protein^{-1}$)		
		Malate-glutamate		Succinate
		− rotenone	+ rotenone	
Control	0.93 ± 0.07	0.40 ± 0.19	0.62 ± 0.12	0.52 ± 0.08
Diabetes	1.14 ± 0.06*	0.91 ± 0.08***	0.95 ± 0.12*	0.62 ± 0.09

* $p < 0.05$; *** $p < 0.005$ Diabetes *vs.* Control group (Studentś *t*-test, n = 6).

Table 5
Mn-SOD activity and concentration (expressed as active center) of heart mitochondria of control and STZ-induced diabetic rats.

Group	Mn-SOD		
	Activity (U mg $protein^{-1}$)	Concentration (μM)	
		Active centers#	Enzyme
Control	143 ± 32	68 ± 9	17 ± 3
Diabetes	71 ± 8*	35 ± 4	8.5 ± 0.9

* $p < 0.05$ Diabetes *vs.* Control group (Student's *t*-test, n = 4).
# The concentration of Mn-SOD active centers was calculated taking into account the value of Mn-SOD activity, the amount of commercial SOD that inhibits 50% ferricytochrome *c* reduction by each SOD unit (1 U SOD corresponds to 4 pmol SOD), the sample protein concentration (0.3–1.0 mg mitochondrial protein ml^{-1}), and a volume of 7.2 μl mitochondrial matrix. mg $protein^{-1}$ (Costa et al., 1988). The concentration of Mn-SOD (μM enzyme) in the mitochondrial matrix was calculated as (μM active center)/4, because mammalian Mn-SOD is a homotetramer with a manganese ion per subunit.

These results suggest an impaired respiratory chain, mainly due to complex I dysfunction, which correlates with the diminished tissue O_2 consumption.

7.3.2. Hydrogen peroxide and nitric oxide production rates

State 4 mitochondrial H_2O_2 production rates were measured using malate-glutamate or succinate as substrates (Table 4). The main impairment of complex I activity was evidenced by the increase in H_2O_2 production rates using malate-glutamate but not succinate as substrates. When malate-glutamate was used, the rate of H_2O_2 released by heart mitochondria from diabetic animals was 127% higher than the one detected from control mitochondria. This results agrees with the impairment observed in electron transfer activities of the complexes involved in O_2^- production; *i.e.* complexes I and III. Moreover, the supplementation of the reaction medium with 1 μM rotenone produced an enhancement in H_2O_2 production rate of about 55% in control mitochondria (0.62 ± 0.12 nmol min^{-1} mg $protein^{-1}$), but only of about 4% in heart mitochondria from diabetic animals (0.95 ± 0.12 nmol min^{-1} mg $protein^{-1}$), suggesting structural modifications of complex I proteins in heart mitochondria from diabetic rats associated to oxidative stress.

In addition, the NO production by heart mitochondrial membranes, *i.e.* mtNOS activity, was significantly increased by 23% in the diabetic group in comparison with control group (Table 4), indicating a higher mtNOS expression in heart mitochondria from diabetic than from control animals.

7.3.3. Mn-SOD activity and active concentration

The activity of Mn-SOD was measured and Mn-SOD concentration in the mitochondrial matrix was calculated (Table 5). Mn-SOD from heart mitochondria of control animals was 143 ± 32 U_{SOD} mg $protein^{-1}$ which corresponds to a Mn-SOD "active" concentration of 68 ± 9 μM expressed as active centres or 17 ± 4 μM expressed as enzyme, in the mitochondrial matrix. In diabetic animals, both Mn-SOD activity and concentration were about 50% lower than in control mitochondria, leading to an enhancement in O_2^- steady-state concentration in the mitochondrial matrix.

7.4. Protein tyrosine nitration

Tyrosine nitration of mitochondrial proteins was analysed by Western Blot using an anti-3-nitrotyrosine antibodies (Fig. 3). Fig. 3B illustrate the densitometric units relative to VDAC-1, this latter used as a loading control. An increase in tyrosine nitration of about 58% was observed in heart mitochondrial proteins from diabetic animals in comparison with control rats, suggesting an enhancement in the generation and/or steady-state concentration of $ONOO^-$. This result agrees with both the increased mitochondrial NO production as the augmented O_2^- steady-state concentration, this latter supported by the enhancement in H_2O_2 production rate and by the reduction in Mn-SOD activity of hearts from diabetic animals.

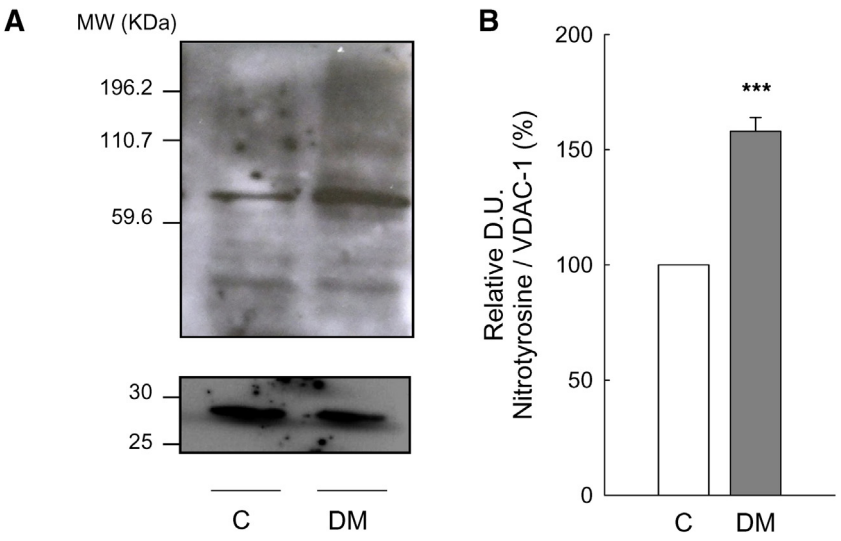

Fig. 3. (A) Western blot analysis of heart mitochondrial membranes using anti-3-nitrotyrosine antibody (upper panel) (HM.11, sc-32731 Santa Cruz Biotechnology, Santa Cruz, CA) and VDAC-1 antibody (lower panel) as loading control (D-16: sc-32063, Santa Cruz Biotech.). (B) Densitometric units ratio between 3-nitrotyrosine and VDAC-1, expressed as the percentage relative to control. *** $p < 0.001$ Diabetes *vs.* Control group (Student's *t*-test, n = 3).

8. Discussion

The results presented in this work provide evidence that STZ-induced diabetic rats did not show cardiac hypertrophy nor alterations in the cardiac performance when their hearts work at resting conditions. However, they exhibited ventricular systolic and diastolic dysfunction when hearts were exposed to a work overload, suggesting a lower capacity of hearts from diabetic than from control rats to respond towards an extra metabolic requirement. The higher time needed to reach 50% of relaxation after isoproterenol addition in hearts from diabetic animals than controls, indicates changes in the lusitropic reserve and suggests variations in Ca^{2+} transients during contraction and relaxation processes (Yu et al., 1994), modifying the correct relaxation of the myocardium in response to β-agonists.

It has been proposed that the failure in the contractile function in response to a work overload might be originated by mitochondrial dysfunction (Beer et al., 2002; How et al., 2006; Neubauer, 2007). In this sense, Anderson et al. (2009) have shown mitochondrial dysfunction in permeabilized muscle cells obtained from human cardiac tissue, providing evidences into the role of mitochondrial dysfunction and oxidative stress in the pathogenesis of heart failure in diabetic patients. In the experimental model used in this article, the decline in O_2 uptake observed in hearts from diabetic animals was produced by changes in active mitochondrial respiration (Tables 1 and 2). Moreover, the decay detected in state 3 O_2 consumption, without changes in state 4 respiration, agrees with the cardiac compromise observed only after a β-adrenergic stimulus. The difference between the resting and the active respiration is known as *mitochondrial reserve capacity* and allows the cardiomyocytes to sustain the correct function of the tissue when the energetic demand is enhanced (Hill et al., 2009). In physiological conditions, only about 30–40% of the maximum ATP production capacity is used (Navarro et al., 2005; Valdez and Boveris, 2007). In addition, lower mitochondrial complexes activities (Table 3) and ADP/O ratio (Table 2) were observed in hearts from diabetic respect to control animals, suggesting an inefficient oxidative phosphorylation. To note, an imbalance between the ATP demand and supply was previously observed in human hearts with cardiac failure, impeding a correct contractile work (Beer et al., 2002; Neubauer, 2007). Taking into account the values of state 3 O_2 consumption and ADP/O ratio, ATP production rate can be estimated, multiplying both data. The oxidative phosphorylation rate was about 588 nmol ATP min^{-1} mg $protein^{-1}$ for control mitochondria *vs.* 389 nmol ATP min^{-1} mg $protein^{-1}$ for mitochondria from diabetic animals, when malate-glutamate was used; and 470 *vs.* 337 nmol ATP. min^{-1} mg $protein^{-1}$, for control and diabetic mitochondria, respectively, when succinate was used as substrate. Therefore, a decrease in ATP production rate of about 34% and 28% (for malate-glutamate and succinate, respectively) was observed in heart mitochondria of diabetic animals. Consequently, the impairment in the oxidative phosphorylation detected in heart from diabetic rats agrees with the changes observed in cardiac performance after isoproterenol addition (Fig. 2).

It is known that H_2O_2 and NO production by mitochondria plays a critical role in Diabetes-related metabolic disorders (Rolo and Palmeira, 2006; Tocchetti et al., 2015). Under our experimental conditions, we observed an increase in H_2O_2 production rate (diabetic *vs.* control animals) only when mitochondria were supplemented with complex I substrates, suggesting structural modifications of complex I proteins in heart from diabetic rats, probably associated to oxidative stress. Not only O_2^- production by complex I–III is enhanced in heart mitochondria of diabetic rats, as evidenced by the increase in H_2O_2 production, but also O_2^- decomposition by SOD-catalysed reaction is decreased, being the Mn-SOD activity declined by about 50%. In this context, O_2^- steady-state concentration in the mitochondrial matrix is increased. These results are consistent with the data obtained in heart from OVE26 transgenic mice that showed both an increase in free radical generation as a decline in antioxidant defences (Shen et al., 2006), involving to oxidative stress in the initiation, progression and pathological consequences of Diabetes (Cai, 2006). To note, complex I provides NAD^+ required for the steady-state operation of the Krebs cycle, and serves as the major entry point for feeding the respiratory chain with the reducing equivalents needed for the electrochemical gradient of H^+ generation and subsequent ATP synthesis. The O_2^- production rate by complex I is increased by inhibition of electron transfer with rotenone (Boveris and Chance, 1973) or by complex I dysfunction (Hensley et al., 2000; Navarro and Boveris, 2009). The concept of "complex I syndrome" was recently described and defined (Boveris et al., 2010), and it is characterized by a decline in tissue O_2 uptake and malate-glutamate-supported mitochondrial respiration, associated to complex I and mtNOS activities impairment, O_2^- and H_2O_2 production rates enhancement, sustained by

complex I substrates, and phospholipid and protein oxidation and protein nitration increments. The molecular mechanism responsible for complex I syndrome is probably accounted by a series of processes and reactions that lead to complex I inactivation (Boveris et al., 2010; Valdez et al., 2011; Vanasco et al., 2012).

Additionally, an enhancement in NO production by mtNOS (23%) was observed in heart of diabetic animals respect to control. The enhancement in mitochondrial NO production together with the increase in O_2^- steady-state concentration agrees with the enhancement of protein tyrosine nitration (58%) observed in heart mitochondria of diabetic rats (Fig. 3). These data support the idea that in pathological situations in which Mn-SOD activity is reduced, the metabolic pathway between O_2^- and NO is exacerbated increasing $ONOO^-$ generation (Bombicino et al., 2016a; Valdez et al., 2016). In addition, considering that approximately 40–50% of the NO might be produced in the mitochondria and diffused to the cytosol (Valdez et al., 2004; Zaobornyj et al., 2009), this molecule may play a central role as mitochondrion-cytosol signalling. Mitochondrial NO could diffuse to the cytosol and participate in the excitation-contraction coupling, through cGMP dependent pathways (Balligand et al., 1993; Kaye et al., 1996; Tao and McKenna, 1994), explaining the contractile dysfunction observed in the diabetic heart when a β-adrenergic stimulus is applied.

In this context, changes in H_2O_2 and NO production and in energetic mitochondrial states could be communicated to cytosol, inducing a compensatory and/or adaptive response, in which Ca^{2+} homeostasis processes could be involved. It is known that mitochondria regulate cytosolic signalling pathways: (a) they provide ATP to support the cellular energy demands; (b) they generate H_2O_2 and NO, both involving in the modulation of redox-sensitive kinase signalling and transcriptional pathways (*i.e.* the insulin and insulin-like growth factor (IGF-1) signalling and the MAPK pathways, and the cGMP-PKG pathway that activates Sirt1 and PGC-1α); and (c) they participate in $NAD(P)^+$/NAD(P)H homeostasis, which, in turn, influence in mitochondrial biogenesis (Yin et al., 2014). Although more studies are necessary, the enhancement in mitochondrial H_2O_2 and NO production rates observed in heart from diabetic animals may be associated to redox-sensitive signalling modulation and to mitochondrial biogenesis triggering (Bombicino et al., 2016a).

To conclude, the results presented in this article suggest that a sustained hyperglycemia leads to heart mitochondrial dysfunction, in which state 3 O_2 consumption and oxidative phosphorylation efficiency are decreased, and H_2O_2 and NO production rates are increased, producing a cardiac compromise against a work overload. This mitochondrial impairment was detected in the absence of heart hypertrophy and of changes in resting cardiac performance, suggesting that mitochondrial dysfunction could precede the onset of diabetic cardiac failure. Fluctuations in mitochondrial redox (H_2O_2 and NO) and energetic (ATP) states could be part of an intricate network of signalling molecules, involved in the underlying cellular events that lead to the diabetic cardiomyopathy.

Acknowledgments

This work was supported by research grants from the University of Buenos Aires (UBACyT 200-201-101-00140, 200-201-301-00731), Agencia Nacional de Promoción Científica y Tecnológica (ANPCyT, PICT 2014-0964), and Consejo Nacional de Investigaciones Científicas y Técnicas (CONICET; PIP 112-201-101-00444).

References

Anderson, E.J., Kypson, A.P., Rodriguez, E., Anderson, C.A., Lehr, E.J., Neufer, P.D., 2009. Substrate-specific derangements in mitochondrial metabolism and redox balance in the atrium of the type 2 diabetic human heart. J. Am. Cell Cardiol. 54, 1891–1898, http://dx.doi.org/10.1016/j.jacc.2009.07.031.

Antunes, F., Boveris, A., Cadenas, E., 2004. On the mechanism and biology of cytochrome oxidase inhibition by nitric oxide. Proc. Natl. Acad. Sci. U. S. A. 101, 16774–16779.

Antunes, F., Boveris, A., Cadenas, E., 2007. On the biologic role of the reaction of NO with oxidized cytochrome *c* oxidase. Antioxid. Redox Signal. 9, 1569–1579, http://dx.doi.org/10.1089/ars.2007.1677.

Aon, M.A., Tocchetti, C.G., Bhatt, N., Paolocci, N., Cortassa, S., 2015. Protective mechanisms of mitochondria and heart function in Diabetes. Antioxid. Redox Signal. 22, 1563–1586.

Balligand, J.L., Ungureanu, D., Kelly, R.A., Kobzik, L., Pimental, D., Michel, T., Smith, T.W., 1993. Abnormal contractile function due to induction of nitric oxide synthesis in rat cardiac myocytes follows exposure to activated macrophage-conditioned medium. J. Clin. Invest. 91, 2314–2319, http://dx.doi.org/10.1172/JCI116461.

Beer, M., Seyfarth, T., Sandstede, J., Landschutz, W., Lipke, C., Köstler, H., von Kienlin, M., Harre, K., Hahn, D., Neubauer, S., 2002. Absolute concentrations of high-energy phosphate metabolites in normal, hypertrophied, and failing human myocardium measured noninvasively with 31P-SLOOP magnetic resonance spectroscopy. J. Am. Coll. Cardiol. 40, 1267–1274, http://dx.doi.org/10.1016/S0735-1097(02)02160-5.

Belke, D.D., Larsen, T.S., Gibbs, E.M., Severson, D.L., 2001. Glucose metabolism in perfused mouse hearts overexpressing human GLUT-4 glucose transporter. Am. J. Physiol. Endocrinol. Metab. 280, E420–E427.

Bombicino, S.S., Iglesias, D.E., Rukavina Mikusic, I.A., Boveris, A., Valdez, L.B., 2016a. Heart mitochondrial dysfunction in diabetic rats. Biocell 39, 7–10.

Bombicino, S.S., Zaobornyj, T., Iglesias, D.E., Boveris, A., Valdez, L.B., 2016b. Mitochondrial nitric oxide production supported by reverse electron transfer. Arch. Biochem. Biophys. 607, 8–19.

Boudina, S., Dale Abel, E., 2007. Diabetic cardiomyopathy revisited. Circulation 115, 3213–3223, http://dx.doi.org/10.1161/CIRCULATIONAHA.106.679597.

Boveris, A., Cadenas, E., 1975. Mitochondrial production of superoxide anion and its relationship to the antimycin insensitive respiration. FEBS Lett. 54, 311–314, http://dx.doi.org/10.1016/0014-5793(75)80928-8.

Boveris, A., Chance, B., 1973. The mitochondrial generation of hydrogen peroxide. Biochem. J. 134, 617–630.

Boveris, A., Oshino, N., Chance, B., 1972. The cellular production of hydrogen peroxide. General properties and effect of hyperbaric oxygen. Biochem. J. 128, 707–716, PMCID: PMC1177867.

Boveris, A., Costa, L.E., Cadenas, E., Poderoso, J.J., 1999. Regulation of mitochondrial respiration by adenosine diphosphate, oxygen and nitric oxide. Methods Enzymol. 301, 188–198, http://dx.doi.org/10.1016/S0076-6879(99)01082-4.

Boveris, A., Lores Arnaiz, S., Bustamante, J., Alvarez, S., Valdez, L.B., Boveris, A.D., Navarro, A., 2002. Pharmacological regulation of mitochondrial nitric oxide synthase. Methods Enzymol. 359, 328–339.

Boveris, A., Valdez, L.B., Zaobornyj, T., Bustamante, J., 2006. Mitochondrial metabolic states regulate nitric oxide and hydrogen peroxide diffusion to the cytosol. Biochim. Biophys. Acta 1757, 535–542, http://dx.doi.org/10.1016/j.bbabio.2006.02.010.

Boveris, A., Carreras, M.C., Poderoso, J.J., 2010. The regulation of cell energetics and mitochondrial signaling by nitric oxide. In: Ignarro, L. (Ed.), Nitric Oxide. Elsevier Academic Press, London, pp. 441–482.

Boveris, A., 1984. Determination of the production of superoxide radicals and hydrogen peroxide in mitochondria. Methods Enzymol. 105, 429–435, PMID: 6328196.

Brown, G.C., Cooper, C.E., 1994. Nanomolar concentrations of nitric oxide reversibly inhibit synaptosomal respiration by competing with oxygen at cytochrome oxidase. FEBS Lett. 356, 295–298, http://dx.doi.org/10.1016/0014-5793(94)01290-3.

Brownlee, M., 1995. The pathological implications of protein glycation. Clin. Invest. Med. 18, 275–281, PMID: 8549013.

Bugger, H., Boudina, S., Hu, X.X., Tuinei, J., Zaha, V.G., Theobald, H.A., Yun, U.J., McQueen, A.P., Wayment, B., Litwin, S.E., Abel, E.D., 2008. Type 1 Diabetic Akita mouse hearts are Insulin sensitive but manifest structurally abnormal mitochondria that remain coupled despite increased uncoupling Protein 3. Diabetes 57, 2924–2932, http://dx.doi.org/10.2337/db08-0079.

Bustamante, J., Bersier, G., Aron-Badin, R., Cymeryng, C., Parodi, A., Boveris, A., 2002. Sequential NO production by mitochondria and endoplasmic reticulum during induced apoptosis. Nitric Oxide: Biol. Chem. 6, 333–341, http://dx.doi.org/10.1006/niox.2001.0420.

Cai, L., 2006. Suppression of nitrative damage by metallothionein in diabetic heart contributes to the prevention of cardiomyopathy. Free Radic. Biol. Med. 41, 851–861, http://dx.doi.org/10.1016/j.freeradbiomed.2006.06.007.

Cleeter, M.W., Cooper, J.M., Darley-Usmar, V.M., Moncada, S., Schapira, A.H., 1994. Reversible inhibition of cytochrome c oxidase, the terminal enzyme of the mitochondrial respiratory chain, by nitric oxide. Implications for neurodegenerative diseases. FEBS Lett. 345, 50–54, http://dx.doi.org/10.1016/0014-5793(94)00424-2.

Costa, L.E., Boveris, A., Koch, O.R., Taquini, A.C., 1988. Liver and Heart mitochondria in rats submitted to chronic hypobaric hypoxia. Am. J. Physiol. 255, C123–C129, PMID: 2839034.

Elfering, S.L., Sarkela, T.M., Giulivi, C., 2002. Biochemistry of mitochondrial nitric-oxide synthase. J. Biol. Chem. 277, 38079–38086, http://dx.doi.org/10.1074/jbc.M205256200.

Ernster, L., 1986. Oxygen as an environmental poison. Chem. Scripta 26, 525–534.

Estabrook, R.W., 1967. Mitochondrial respiratory control and the polarographic measurement of ADP:O ratios. Methods Enzymol. X, 41–47.
Ferreira, F.M., Palmeira, C.M., Seica, R., Moreno, A.J., Santos, M.S., 2003. Diabetes and mitochondrial bioenergetics: alterations with age. J. Biochem. Mol. Toxicol. 17, 214–222, http://dx.doi.org/10.1002/jbt.10081.
Fitzl, G., Welt, K., Wassilew, G., Clemens, N., Penka, K., Mukke, N., 2002. The influence of hypoxia on the myocardium of experimentally diabetic rats with and without protection by Ginkgo biloba extract. III. Ultrastructural investigations on mitochondria. Exp. Toxicol. Pathol. 52, 557–568, http://dx.doi.org/10.1016/S0940-2993(01)80017-8.
Flohe, L., Gunzler, W.A., 1984. Assays of glutathione peroxidase. Methods Enzymol. 105, 114–121, PMID: 6727659.
Giulivi, C., Poderoso, J.J., Boveris, A., 1998. Production of nitric oxide by mitochondria. J. Biol. Chem. 273, 11038–11043, http://dx.doi.org/10.1074/jbc.273.18.11038.
Giulivi, C., 1998. Functional implications of nitric oxide produced by mitochondria in mitochondrial metabolism. Biochem. J. 332, 673–679, PMCID: PMC1219527.
Hatefi, Y., 1985. The mitochondrial electron transport and oxidative phosphorylation system. Annu. Rev. Biochem. 54, 1015–1069, http://dx.doi.org/10.1146/annurev.bi.54.070185.005055.
Hensley, K., Kotake, Y., Sang, H., Pye, Q.N., Wallis, G.L., Kolker, L.M., Tabatabaie, T., Stewart, C.A., Konishi, Y., Nakae, D., Floyd, R.A., 2000. Dietary choline restriction causes complex I dysfunction and increased H_2O^2 generation in liver mitochondria. Carcinogenesis 21, 983–989.
Hill, B.G., Dranka, B.P., Zou, L., Chatham, J.C., Darley-Usmar, V.M., 2009. Importance of the bioenergetic reserve capacity in response to cardiomyocyte stress induced by 4-hydroxynonenal. Biochem. J. 424, 99–107, http://dx.doi.org/10.1042/BJ20090934.
How, O.J., Aasum, E., Severson, D.L., Chan, W.Y., Essop, M.F., Larsen, T.S., 2006. Increased myocardial oxygen consumption reduces cardiac efficiency in diabetic mice. Diabetes 55, 466–473, http://dx.doi.org/10.2337/diabetes.55.02.06, db05-1164.
Iglesias, D.E., Bombicino, S.S., Valdez, L.B., Boveris, A., 2015. Nitric oxide interacts with mitochondrial complex III producing antimycin-like effects. Free Radical Biol. Med. 89, 602–613, http://dx.doi.org/10.1016/j.freeradbiomed.2015.08.024.
Jain, M., Lim, C.C., Nagata, K., Davis, V.M., Milstone, D.S., Liao, R., Mortensen, R.M., 2001. Targeted inactivation of Gαi does not alter cardiac function or β-adrenergic sensitivity. Am. J. Physiol. Heart Circ. Physiol. 208, H569–H575, PMID: 11158953.
Joffe, I.I., Travers, K.E., Perreault-Micale, C.L., Hampton, T., Katz, S.E., Morgan, J.P., Douglas, P.S., 1999. Abnormal cardiac function in the streptozotocin-induced, non-insulin-dependent diabetic rats: non-invasive assessment with doppler echocardiography and contribution of the nitric oxide pathway. J. Am. Coll. Cardiol. 34, 2111–2119, http://dx.doi.org/10.1016/S0735-1097(99)00436-2.
Jones, D.P., Sies, H., 2015. The redox code. Antioxid. Redox Signal. 23, 734–746, http://dx.doi.org/10.1089/ars.2015.6247.
Kaye, D.M., Wiviott, S.D., Balligand, J.L., Simmons, W.W., Smith, T.W., Kelly, R.A., 1996. Frequency-dependent activation of a constitutive nitric oxide synthase and regulation of contractile function in adult rat ventricular myocytes. Circ. Res. 78, 217–224, http://dx.doi.org/10.1161/01.RES.78.2.217.
Kissner, R., Nauser, T., Bugnon, P., Lye, P.G., Koppenol, W.H., 1997. Formation and properties of peroxynitrite as studied by laser flash photolysis, high-pressure stopped-flow technique and pulse radiolysis. Chem. Res. Toxicol. 10, 1285–1292, http://dx.doi.org/10.1021/tx970160x.
Li, C.J., Zhang, Q.M., Li, M.Z., Zhang, J.Y., Yu, P., Yu, D.M., 2009. Attenuation of myocardial apoptosis by alpha-lipoic acid through suppression of mitochondrial oxidative stress to reduce diabetic cardiomyopathy. Chin. Med. J. (Engl.) 122, 2580–2586, PMID: 19951573.
Lowry, O.H., Rosebrough, N.J., Farr, A.L., Randall, R.J., 1951. Protein measurement with the Folin phenol reagent. J. Biol. Chem. 193, 265–275, PMID: 14907713.
Marchini, T., Magnani, N., D'Annunzio, V., Tasat, D., Gelpi, R.J., Alvarez, S., Evelson, P., 2013. 2013. Impaired cardiac mitochondrial function and contractile reserve following an acute exposure to environmental particulate matter. Biochim. Biophys. Acta 1830, 2545–2552, http://dx.doi.org/10.1016/j.bbagen.2012.11.012.
McCord, J.M., Fridovich, I., 1969. Superoxide dismutase. An enzymic function for erythrocuprein (hemocuprein). J. Biol. Chem. 244, 6049–6055, PMID: 5389100.
Mela, I., Seitz, S., 1979. Isolation of mitochondria with emphasis on heart mitochondria from small amounts of tissue. Meth. Enzymol. 55, 39–46, PMID: 459851.
Mora, A.C., Aragón, D.M., Ospina, L.F., 2009. Oxidative stress characterization in streptozotocin-diabetic wistar rats. VITAE. Rev. Facultad Quím. Farm. 16, 311–319 (ISSN: 0121-4004).
Murphy, M.E., Noack, E., 1994. Nitric oxide assay using the hemoglobin method. Methods Enzymol. 233, 240–250, http://dx.doi.org/10.1016/S0076-6879(94)33027-1.
Navarro, A., Boveris, A., 2009. Brain mitochondrial dysfunction and oxidative damage in Parkinson's disease. J. Bioenergy Biomembr. 41, 517–521.
Navarro, A., Torrejon, R., Bandez, M.J., Lopez-Cepero, J.M., Boveris, A., 2005. Mitochondrial function and mitochondria-induced apoptosis in an overstimulated rat ovarian cycle. Am. J. Physiol. Endocrinol. Metab. 289, E1101–1109, http://dx.doi.org/10.1152/ajpendo.00223.2005.
Neubauer, S., 2007. The failing heart-an engine out of fuel. N. Engl. J. Med. 356, 1140–1151, http://dx.doi.org/10.1056/NEJMra063052.
Pesta, D., Gnaiger, E., 2012. High-resolution respirometry: OXPHOS protocols for human cells and permeabilized fibers from small biopsies of human muscle. Methods Mol. Biol. 810, 25–58, http://dx.doi.org/10.1007/978-1-61779-382-0_3.
Pierce, G.N., Dhalla, N.S., 1985. Heart mitochondrial function in chronic experimental diabetes in rats. Can. J. Cardiol. 1, 48–54, PMID: 2996724.
Poderoso, J.J., Carreras, M.C., Lisdero, C., Riobó, N., Schöpfer, F., Boveris, A., 1996. Nitric oxide inhibits electron transfer and increases superoxide radical production in rat heart mitochondria and submitochondrial particles. Arch. Biochem. Biophys. 328, 85–92, http://dx.doi.org/10.1006/abbi.1996.0146.
Radi, R., Cassina, A., Hodara, R., Quijano, C., Castro, L., 2002. Peroxynitrite reactions and formation in mitochondria. Free Radic. Biol. Med. 33, 1451–1464, http://dx.doi.org/10.1016/S0891-5849(02)01111-5.
Rolo, A.P., Palmeira, C., 2006. Diabetes and mitochondrial function: role of hyperglycemia and oxidative stress. Toxicol. Appl. Pharmacol. 212, 167–178, http://dx.doi.org/10.1016/j.taap.2006.01.003.
Rossini, A.A., Like, A.A., Chick, W.L., Appel, M.C., Cahill Jr., G.F., 1977. Studies of Streptozotocin-induced insulitis and diabetes. Proc. Natl. Acad. Sci. U. S. A. 74, 2485–2489 (PMC432197).
Shen, X., Zheng, S., Metreveli, N.S., Epstein, P.N., 2006. Protection of cardiac mitochondria by overexpression of Mn-SOD reduces diabetic cardiomyopathy. Diabetes 55, 798–805, http://dx.doi.org/10.2337/diabetes.55.03.06, db05–1039.
Sicari, R., Nihoyannopoulos, P., Evangelista, A., Kasprzak, J., Lancellotti, P., Poldermans, D., Voigt, J.U., Zamorano, J.L., 2008. Stress echocardiography expert consensus statement: European Association of Echocardiography (EAE) (a registered branch of the ESC). Eur. J. Echocardiogr. 9, 415–437, http://dx.doi.org/10.1093/ejechocard/jen175.
Sies, H., 2015. Oxidative stress: a concept in redox biology and medicine. Redox Biol. 4, 180–183, http://dx.doi.org/10.1016/j.redox.2015.01.002.
Tao, S., McKenna, T.M., 1994. In vitro endotoxin exposure induces contractile dysfunction in adult rat cardiac myocytes. Am. J. Physiol. 267, H1745–H1752, PMID: 7526711.
Tatoyan, A., Giulivi, C., 1998. Purification and characterization of a nitric-oxide synthase from rat liver mitochondria. J. Biol. Chem. 273, 11044–11048, http://dx.doi.org/10.1074/jbc.273.18.11044.
Tocchetti, C.G., Stanley, B.A., Sivakumaran, V., Bedja, D., O'Rourke, B., Paolocci, N., Cortassa, S., Aon, M.A., 2015. Impaired mitochondrial energy supply coupled to increased H_2O_2 emission under energy/redox stress leads to myocardial dysfunction during Type I diabetes. Clin. Sci. (Lond.) 129, 561–574, http://dx.doi.org/10.1042/CS20150204.
Tomita, M., Mukae, S., Geshi, E., Umetsu, K., Nakatani, M., Katagiri, T., 1996. Mitochondrial respiratory impairment in Streptozotocin-induced Diabetic rats. Jpn. Circ. J. 60, 673–682, http://dx.doi.org/10.1253/jcj.60.673.
Turrens, J.F., Boveris, A., 1980. Generation of superoxide anion by the NADH dehydrogenase of bovine heart mitochondria. Biochem. J 191, 421–427, PMCID: PMC1162232.
Valdez, L.B., Boveris, A., 2007. Mitochondrial nitric oxide synthase, a voltage-dependent enzyme, is responsible for nitric oxide diffusion to cytosol. Front. Biosci. 12, 1210–1219, http://dx.doi.org/10.2741/2139.
Valdez, L.B., Alvarez, S., Lores Arnaiz, S., Schöpfer, F., Carreras, M.C., Poderoso, J.J., Boveris, A., 2000. Reactions of peroxynitrite in the mitochondrial matrix. Free Radic. Biol. Med. 29, 349–356, http://dx.doi.org/10.1016/S0891-5849(00)00301-4.
Valdez, L.B., Zaobornyj, T., Alvarez, S., Bustamante, J., Costa, L.E., Boveris, A., 2004. Heart mitochondrial nitric oxide synthase. Effects of hypoxia and aging. Mol. Aspects Med. 25, 49–59, http://dx.doi.org/10.1016/j.mam.2004.02.008.
Valdez, L.B., Zaobornyj, T., Boveris, A., 2006. Mitochondrial metabolic states and membrane potential modulate mtNOS activity. Biochim. Biophys. Acta 1757, 166–172, http://dx.doi.org/10.1016/j-bbabio.2006.02.013.
Valdez, L.B., Zaobornyj, T., Bombicino, S., Iglesias, D.E., Boveris, A., Donato, M., DíAnnunzio, V., Bucholz, B., Gelpi, R.J., 2011. Complex I syndrome in miocardial stunning and the effect of adenosine. Free Radic. Biol. Med. 51, 1203–1212, http://dx.doi.org/10.1016/j.freeradbiomed.2011.06.007.
Valdez, L.B., Bombicino, S.S., Iglesias, D.E., Rukavina Mikusic, I.A., D'Annunzio, V., 2016. Mitochondrial complex I inactivation after ischemia-reperfusion in the stunned heart. In: Gelpi, R.J., Boveris, A., Poderoso, J.J. (Eds.), Biochemistry of Oxidative Stress. Physiopathology and Clinical Aspects. Springer, New York, USA, August, In press.
Vanasco, V., Magnani, N.D., Cimolai, M.C., Valdez, L.B., Evelson, P., Boveris, A., Alvarez, S., 2012. Endotoxemia impairs heart mitochondrial function by decreasing electron transfer, ATP synthesis and ATP content without affecting membrane potential. J. Bioenergy Biomembr. 44, 243–252, http://dx.doi.org/10.1007/s10863-012-9426-3.
Vittone, L., Mundiña-Weilenmann, C., Mattiazzi, A., Cingolani, H.E., 1974. Phisiologic and Pharmacologic factors that affect myocardial relaxation. J. Pharmacol. Toxicol. Methods 32, 7–18, http://dx.doi.org/10.1016/1056-8719(94)90011-6.
Yin, F., Cadenas, E., 2015. Mitochondria: the cellular hub of the dynamic coordinated network. Antioxid. Redox Signal. 22, 961–964, http://dx.doi.org/10.1089/ars.2015.6313.
Yin, F., Sancheti, H., Cadenas, E., 2012. Mitochondrial thiols in the regulations of cells death pathways. Antioxid. Redox. Signal. 17, 1714–1727, http://dx.doi.org/10.1089/ars.2012.4639.

Yin, F., Boveris, A., Cadenas, E., 2014. Mitochondrial energy metabolism and redox signaling in brain aging and neurodegeneration. Antioxid. Redox. Signal. 20, 353–371, http://dx.doi.org/10.1089/ars.2012.4774.

Yonetani, T., Ray, G.S., 1965. Studies on Cytochrome Oxidase: VI. Kinetics of the aerobic oxidation of ferrocytochrome *c* by cytochrome oxidase. J. Biol. Chem. 240, 3392–3398.

Yonetani, T., 1967. Cytochrome oxidase: beef heart. Methods Enzymol. 10, 332–335, http://dx.doi.org/10.1016/0076-6879(67)10062-1.

Yu, Z., Quamme, G.A., McNeill, J.H., 1994. Depressed $[Ca_2]_i$ responses to isoproterenol and cAMP in isolated cardiomyocytes from experimental diabetic rats. Am. J. Physiol. 266, H2334–H2342, PMID: 8023994.

Zaobornyj, T., Valdez, L.B., Iglesias, D.E., Gasco, M., Gonzales, G., Boveris, A., 2009. Mitochondrial nitric oxide metabolism during rat heart adaptation to high altitude: effect of sildenafil, L-NAME and L-arginine treatments. Am. J. Physiol. Heart Circ. Physiol. 296, 1741–1747, http://dx.doi.org/10.1152/ajpheart.00422.2008.